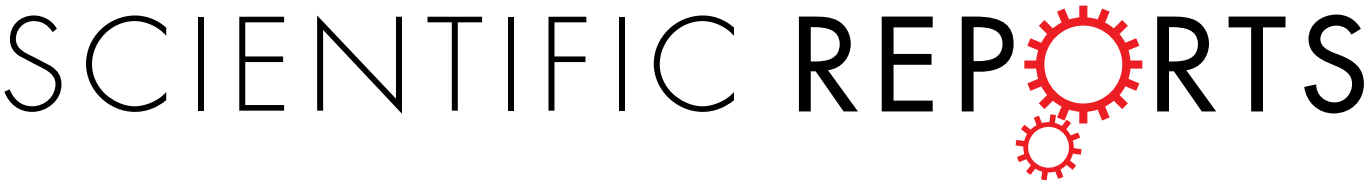

OPEN

Bell's inequality tests via correlated diffraction of high-dimensional position-entangled two-photon states

Received: 11 September 2017
Accepted: 8 March 2018
Published online: 19 March 2018

Wei Li[1,3] & Shengmei Zhao[1,2]

Bell inequality testing, a well-established method to demonstrate quantum non-locality between remote two-partite entangled systems, is playing an important role in the field of quantum information. The extension to high-dimensional entangled systems, using the so-called Bell-CGLMP inequality, points the way in measuring joint probabilities, the kernel block to construct high dimensional Bell inequalities. Here we show that in theory the joint probability of a two-partite system entangled in a Hilbert space can be measured by choosing a set of basis vectors in its dual space that are related by a Fourier transformation. We next propose an experimental scheme to generate a high-dimensional position-entangled two-photon state aided by a combination of a multiple-slit and a 4 f system, and describe a method to test Bell's inequality using correlated diffraction. Finally, we discuss in detail consequences of such Bell-test violations and experimental requirements.

Entanglement, the superposition of multi-particle product states, is one of the most fascinating properties of quantum mechanics[1,2]. Not only has it enriched our knowledge of fundamental physics, it has also been applied with success in the transmission of quantum information. To date, theoretical research and practical applications have both mainly focused on two-photon polarization entanglement[3–7] as two-dimensional entanglement ($2D$) is easy to generate and modulate. Researching high-dimensional entanglement has aroused wide research interest[8–10] because of its critical role in fundamental quantum physics and emergent quantum information technology[11–13]. For instance, higher degrees of freedom enable a single photon to carry more information and thus denser coding[14–17]. Moreover, high-dimensional entangled quantum systems manifest stronger violations of local realism theories than $2D$ systems[18] and are less vulnerable to environment noise. In terms of security, a quantum-key-distribution protocol based on multi-dimensional entanglement has been proven to be more effective against a symmetric attack[19]. In addition, investigations of high dimensional entanglement would also benefit the understanding of quantum teleportation, a key element in quantum computing[20].

Conducting quantum information tasks needs the proof of quantum non-locality of the source, which is accomplished through entanglement witnesses such as tests of Bell's inequality. One of the most famous formulations of Bell's inequality was developed by Collins, Gisin, Linden, Massar and Popescu (CGLMP) with the objective of describing high-dimensional quantum entangled two-partite systems[21], it has been successfully applied to various physical systems[8–10]. The operational principle underlying Bell-CGLMP inequality tests can be described as follows. Assume there is a D-dimensional quantum entangled two-partite systems shared by the two remotely separated participants, Alice and Bob. Alice and Bob individually take two different measurements (A_1, A_2 and B_1, B_2) on their respective systems, and then receives D possible results for each measurement: A_1, A_2 and B_1, $B_2 = 0, 1, 2, \ldots, D-1$. Different measurements are characterized by measurement parameters (α_a, β_b with $a, b = 0,1$), for example the rotation angle of a polarizer for polarization entanglement[1,22], the change in computer-generated holograms for orbital angular momentum entanglement[9,23,24] or the time-delay for time-bin entanglement[25]. With enough measurements, the joint probabilities $P(A_a, B_b)$ can be calculated, and are the building blocks for the construction of the Bell function I_D. If the correlated system can be described by local realism

[1]Nanjing University of Posts and Telecommunications, Institute of Signal Processing and Transmission, Nanjing, 210003, China. [2]Nanjing University of Posts and Telecommunications, Key Lab Broadband Wireless Communication and Sensor, Network, Ministy of Education, Nanjing, 210003, China. [3]Sunwave Communications CO, Hangzhou, 310053, China. Correspondence and requests for materials should be addressed to W.L. (email: alfred_wl@njupt.edu.cn)

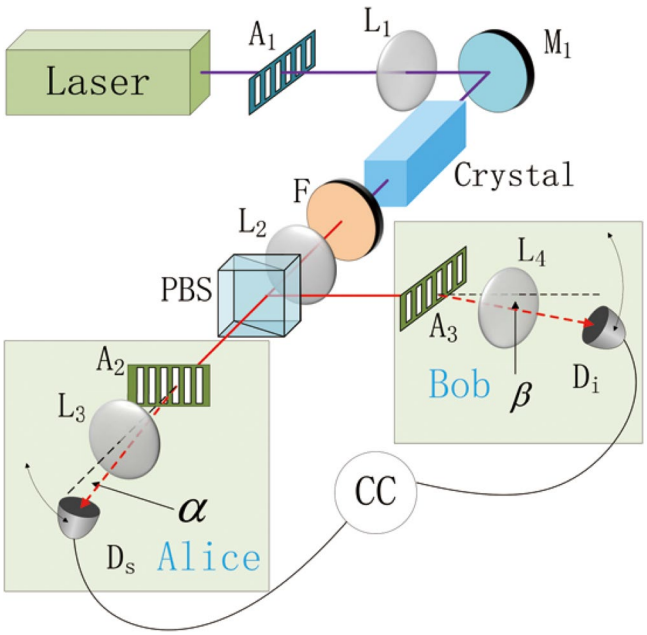

Figure 1. Schematic of the of the optical arrangements for the generation of *D*-dimensional position-entangled two photon state. The plane-wave like pump beam emitted from a quasi-monochromatic laser is transmitted through an opaque plate A_1, a *D*-fold slits, in which the distance between two adjacent slits is *l*, then are divided into *D* even-distributed parts in the transverse plane. A 4*f* optical system comprising lenses L_1 and L_2 focuses the pump beam onto a nonlinear crystal to generate a frequency degenerate type-*II* SPDC, and the transverse plane of the down-converted signal and idler beams are inverted at the output surface of L_2. The remainder pump beam is then filtered by a band-pass filter (F). The signal and idler beams are separated by a polarization beam splitter (PBS) and then transported to slits A_1 and A_2 to undergo diffraction. The diffracted single-photon states are focused by lenses L_3, L_4, and then collected by single-photon detectors D_1 and D_2. The counts are sent to a coincidence circuit to obtain the joint probability.

theorems, then I_D is no larger than 2, whereas if the correlated system is described by quantum theory, then the inequality will be violated. This is the way we test for quantum non-locality.

The development of high-dimensional quantum information has been stimulated by the experimental generation of multidimensional entanglement. The most widely used methods of generating a high-dimensional bi-partite entanglement depend on spontaneous parametric down-conversion (SPDC) by exploring certain degrees of freedom, such as orbital angular momentum[9,24,26], angular position[23], momentum[27–29], position[30–32], time-bin[25,33] and frequency[34–36]. These methods actually depend on phase-matching during SPDC[37], all of which stem from momentum entanglement. A series of impressive work conducted by S. Pádua and collaborators showed that the angular spectrum of the pump beam can be transferred to the joint probability distribution of the down-converted photons[38], and maximally entangled states can be generated in position space by transmitting the pump beam through a multi-slit array[39,40]. However, in their work, a Bell inequality, which is a physical way to eliminate all classical correlations that could be described by any local realism theorem, has not been tested for these high-dimensional position-entangled two-photon states.

In this paper, based on the experimental configuration describe in Pádua *et al.*[40], we suggest a 4*f* system to generate a *D*-dimensional position-entangled two-photon state and propose a method to measure the quantum correlations to construct the Bell-CGSLM inequality. Using the Fourier transformation, we show that a high-dimensional two-photon state entangled in single Hilbert space (position space) also has an entanglement behaviour in its dual space (momentum space). The joint probability for the position-entangled two-photon state, which is the elemental building block of Bell-CGLMP inequality tests, can be calculated by taking a set of measurements with basis vectors in momentum space. We show that the violation of Bell-CGMLP inequality can be obtained by detecting the correlated diffraction, which actually is an interference of multiple-slits diffraction, and the influence of the single-slit diffraction can be suppressed by selecting an appropriate ratio between the distance of neighbouring slits and the width of the slit.

Theoretical scheme

The schematic diagram of our proposal is shown in Fig. 1. A chromatic plane wave like pump beam is divided into *D* parts in the transverse plane by an opaque plate A_1, composed of D-fold slits separated by a distance *l*. A similar experiment was first realized by Monken *et al.*[38]. The structured pump beam is focused onto a collinear type-*II* nonlinear crystal by lens L_1, and the output beam is then collimated by lens L_2. Here the lenses L_1 and L_2 comprise a 4 *f* system with A_1 lying within the first focal plane of L_1. The co-linearly down-converted photon pairs are then imaged on the second focal plane of L_2 with a same but inverse transverse dimension as the opaque plate A_1. The remaining pump beam is filtered by a band-pass filter *F*. The signal and idler photons with orthogonal

polarizations are spatially separated by a polarization beam splitter (PBS), and then directed to the two identical D-fold slits A_2 and A_3 possessed by Alice and Bob, respectively. In this proposed experimental setup, A_2 and A_3 locate at the second focal plane of L_2. A_1, A_2 and A_3 have exactly the same number of slits as well as the adjacent slit separation, while the width of each slit in A_2 and A_3 is much smaller then that of A_1. The lenses L_3 and L_4, located behind A_2 and A_3, direct the diffracted photon states to single-photon detectors D_1 and D_2, scanning along the focal planes of L_3 and L_4. The counts from D_1 and D_2 are sent to a coincidence circuit to output the joint probability. Note that, in previous works[38,40], in order to generate the spatial entanglement, only one focal lens is emplyed in the light path. As a consequence, the transverse dimension of the two-photon state will increase for a longer propagation distance. While our proposed 4*f* imaging system guarantees that the transverse spatial dimension of the down-converted two-photon state remains the same as that of the pump beam, which makes the arrangement of A_2 and A_3 easier. The precise transverse alignment between A_2 and A_3 can be achieved by finding a maximal coincidence count between Alice and Bob.

Theoretical analysis

Assuming the incoming pump beam is a plane wave with uniform distribution of the amplitude on the transverse plane, the electromagnetic field of the pump beam after the slits A_1 becomes

$$\mathbf{E}_p(\mathbf{r}) = \frac{1}{\sqrt{D}}\sum_{j=0}^{D-1}\int d\mathbf{s}\cdot\mathbf{E}_p\left(\mathbf{r}_j+\mathbf{s}\right). \tag{1}$$

Here $\mathbf{E}_p\left(\mathbf{r}_j+\mathbf{s}\right)$ is the corresponding electromagnetic field of the pump beam within the j-th slit of the plate A_1, $\mathbf{r}_j$ the centre position of the j-th slit, and $\boldsymbol{s}$ the position vector along the width direction of the slits ranging from $-\mathbf{d}/2$ to $\mathbf{d}/2$. As the width of the slit is far larger than the wavelength, the diffraction effect after A_1 is negligible. The lens L_1 introduces a spherical phase to the structured pump beam, leading to different slit states with different momentum, i.e., $\mathbf{E}_p(\mathbf{k}) = \frac{1}{\sqrt{D}}\sum_{j=0}^{D-1}\int d\mathbf{q}_p\cdot\mathbf{E}_p\left(\mathbf{k}_j+\mathbf{q}_p\right)$ with $\mathbf{q}_p$ the transverse momentum of the pump beam along the width of the slits.

Very intense incident pump field can be treated classically. Hence, with using the paraxial approximation, the two-photon state generated in degenerate SPDC within the nonlinear crystal can be described as

$$|\Psi\rangle = \frac{1}{\sqrt{D}}\sum_{j=0}^{D-1}\int d\mathbf{q}_p\int d\mathbf{q}_s\int d\mathbf{q}_i\hat{a}_s^{+}\left(\frac{\mathbf{k}_j}{2}+\mathbf{q}_s\right)\hat{a}_i^{+}\left(\frac{\mathbf{k}_j}{2}+\mathbf{q}_i\right)\mathbf{E}_p\left(\mathbf{k}_j+\mathbf{q}_p\right)\delta\left(\mathbf{q}_p-\mathbf{q}_s-\mathbf{q}_i\right)\delta(\mathbf{q}_s-\mathbf{q}_i)|0\rangle. \tag{2}$$

Here $\hat{a}_s^{+}\left(\mathbf{k'}_j\right)$, $\hat{a}_i^{+}\left(\mathbf{k'}_j\right)$ are the creation operators for the signal and idler states of the j-th slit. In this equation, the default condition is that the efficiency for SPDC within this momentum range is constant.

After filtering the pump beam, the momentum-entangled down-converted two-photon state at the output surface of the lens L_2 is given by

$$|\Psi\rangle = \frac{1}{\sqrt{D}}\sum_{j=0}^{D-1}|j\rangle_A|j\rangle_B. \tag{3}$$

With an inverse spherical phase introduced by lens L_2, the momentum-entangled two-photon state now is converted into a D-dimensional position-entangled state. Then equation (3) now serves as a position-entangled two-photon state, in which $|j\rangle_A$ and $|j\rangle_B$ are the single photon states corresponding to the j-th slit, i.e., $\int d\mathbf{s}\left|\mathbf{E}_s\left(\mathbf{r}_j+\mathbf{s}\right)\right\rangle_A$ and $\int d\mathbf{s}\left|\mathbf{E}_i\left(\mathbf{r}_j+\mathbf{s}\right)\right\rangle_B$, received by Alice and Bob, respectively. Here we emphasize that the entanglement between the transverse position variables of the signal photon and the idler photon from the same slit is negligible; it is determined by the phase-matching condition and the Heisenberg uncertainty principle. Furthermore, note that light paths, for example at the laboratory stage, the crosstalk between neighbouring slit states due to diffraction effect could be reduced by adjusting the width of the slits in A_1.

As any two of these single-slit photon states $|j\rangle$ do not overlap in the transverse plane, all these photon states constitute a complete set of orthogonal basis vectors. The advantage of this optical arrangement is that with the introduction of a 4*f* system in the SPDC process, the spatial extension of the down-converted photon pairs in the transverse plane is the same as the pump beam, which is easily to dealt with by the down-converted two-photon state. Using a finite-dimensional discrete-Fourier-like transformation, the form of equation (3) reads

$$|\Psi\rangle = \frac{1}{\sqrt{D}}\sum_{k=0}^{D-1}\left[\sum_{j=0}^{D-1}\frac{1}{\sqrt{D}}e^{i\frac{(k+\alpha)j\cdot 2\pi}{D}}|j\rangle_A\right]\left[\sum_{j'=0}^{D-1}\frac{1}{\sqrt{D}}e^{-i\frac{(k+\alpha)j'\cdot 2\pi}{D}}|j'\rangle_B\right] = \frac{1}{\sqrt{D}}\sum_{k=0}^{D-1}|\alpha_k\rangle_A|-\alpha_k\rangle_B. \tag{4}$$

Here, the states $|j\rangle$ and $|\alpha_k\rangle$ are connected by a finite-dimensional discrete Fourier transformation, and the integer variables l, k are the eigenvalues of the state $|j\rangle$ and $|\alpha_k\rangle$ with respect to certain operators. This transformation plays an important role in quantum entanglement, as it relates time-bin entanglement to frequency entanglement[25,41], orbital angular momentum entanglement to angular entanglement[9,23], and momentum entanglement to position entanglement[28,38].

The transformation in equation (4) also plays a vital role deriving the Bell-CGLMP inequality. The quantum correlation between the D-dimensional position-entangled two-photon pairs is detected based on the theoretical work of Collins *et al.*[21], in which the measurement basis vectors selected by Alice and Bob are

$$|k\rangle_{A,a} = \frac{1}{\sqrt{D}}\sum_{j=0}^{D-1} e^{i\frac{(k+\alpha_a)\cdot j}{D}\cdot 2\pi}|j\rangle_A,$$
$$|k'\rangle_{B,b} = \frac{1}{\sqrt{D}}\sum_{j=0}^{D-1} e^{i\frac{(k'+\beta_b)\cdot j}{D}\cdot 2\pi}|j\rangle_B. \quad (5)$$

Here α_a and β_b are the measurement parameters of Alice and Bob with $a, b = 1, 2$ and $\alpha_1 = 0$, $\alpha_2 = 1/2$, $\beta_1 = 1/4$, $\beta_2 = -1/4$. $|k\rangle_{A,a}$ and $|k'\rangle_{B,b}$ are the $k(k')$ -th measurement basis vectors of Alice and Bob, $k(k') = 0, 1, \ldots, D-1$. The measurement basis vectors in equation (5) are just those transformed from $|\alpha_k\rangle$ and $|\beta_{k'}\rangle$ in equation (4). Accordingly, an inference can be drawn that the correlation of the two-partite systems in the Bell-CGMLP test can be measured in its dual space.

By taking the inner product between the measurement basis vectors in equation (5) and the entangled state in equation (3), we calculate the joint probability $p(A_a = k, B_b = k')$ in the following form

$$p(A_a = k, B_b = k') = \frac{1}{D^3}\frac{\sin^2[\pi(k + \alpha_a + k' + \beta_b)]}{\sin^2\left[\frac{\pi}{D}(k + \alpha_a + k' + \beta_b)\right]}. \quad (6)$$

As position and momentum are conjugate variables connected by a Fourier transformation, we can assert from equation (4) that for position-entangled two-photon states the measurement of the joint probability of the entanglement can be accomplished by detecting the correlated diffraction. Accounting for single-slit diffraction, each slit state $|j\rangle$ can be written in the momentum representation as

$$|j\rangle = \int d\theta A(\theta)|\theta\rangle_j. \quad (7)$$

Here, θ is the propagation direction for the photon state in momentum space, λ the wavelength, and $A(\theta)$ the amplitude for $|\theta\rangle_j$, which is a $\sin c$ function of $d\sin c(d\sin\theta/\lambda)$ with d the width of each slit for A_2 and A_3 (Fig. 1). By substituting equation (7) into equation (3), the joint probability density $p(\alpha, \beta)$ for detecting a diffracted photon propagating in the direction α with respect to the normal of A_2 of Alice's system and detecting the diffracted photon propagating in the direction of β with respect to the normal of A_3 of Bob's system now reads

$$p(\alpha, \beta) \propto A^2(\alpha)A^2(\beta)\cdot\frac{1}{D^3}\cdot\frac{\sin^2\left[\frac{\pi}{\lambda}lD(\sin\alpha + \sin\beta)\right]}{\sin^2\left[\frac{\pi}{\lambda}l(\sin\alpha + \sin\beta)\right]}. \quad (8)$$

Here, $A(\alpha)$ and $A(\beta)$ are the components arising from single-slit diffraction and viewed as scale factors, and l is the distance between the centres of two adjacent slits.

There are two main differences between equations (6) and (8): the first is that the joint probability in equation (6) is given for discrete variables whereas that in equation (8) is given for continuous variables, in which case the photon number is not conserved, and the second is that a scale factor $A^2(\alpha)A^2(\beta)$ appears in equation (8) that stems from single-slit diffraction. In actual experiments, the joint probability is obtained by counting a sufficient number of photons. Therefore, only the sum of the variables, such as $k + \alpha_a + k' + \beta_b$ and $\sin\alpha + \sin\beta$, makes sense, making the first difference negligible. The scale factor $A^2(\alpha)A^2(\beta)$ influences the maximal value that we obtain for the Bell function I_D, and this can be overcome by modulating the ratio between the distance of two adjacent slits l and the width of the slit d.

Because equations (6) and (8) are equivalent, a set of $\alpha_{k,a}$ and $\beta_{k',b}$ can be chosen

$$\frac{lD}{\lambda}\sin\alpha_{k,a} = k + \alpha_a,\ \ \frac{lD}{\lambda}\sin\beta_{k',b} = k' + \beta_b \quad (9)$$

When l is much larger than λ, we have on imposing paraxial approximation

$$\alpha_{k,a} = \frac{\lambda}{lD}(k + \alpha_a),\ \ \beta_{k',b} = \frac{\lambda}{lD}(k' + \beta_b) \quad (10)$$

This means that by setting a correlated diffraction in these angles, we obtain the joint probability to construct the Bell-CGLMP inequality.

The joint probability $p(\alpha, \beta)$ for a 5-D position-entangled two-photon state (Fig. 2) is obtained by fixing the measurement angle of Bob's system and scanning that of Alice's. Here the relevant parameter settings are: the wavelength of signal and idler beam 1550 nm, $l = 2$ mm, and $d = 0.2$ mm. The values of the measurement parameters $\beta_b (b = 1, 2)$ chosen by Bob are $\frac{1}{4}$ and $-\frac{1}{4}$, respectively, in Fig. 2(a) and (b), and the five measurement angles for Bob are $\frac{\lambda}{lD}\left(k' \pm \frac{1}{4}\right)$, with $k' = -2, -1, 0, 1, 2$. From Fig. 2, a change in the measurement angle for Bob shifts the correlated diffraction pattern. This is entirely a correlation phenomenon that has been seen both in quantum[32,42] and classical correlations[43]. The sum of all five correlated diffraction curves [Fig. 2(a,b); purple dash-dot curve] smears the interference pattern, a phenomena that has also been reported in quantum ghost interference[32,44–46]. From single-slit diffraction, the amplitude of the correlated diffraction tends to decrease as the measurement angle increases.

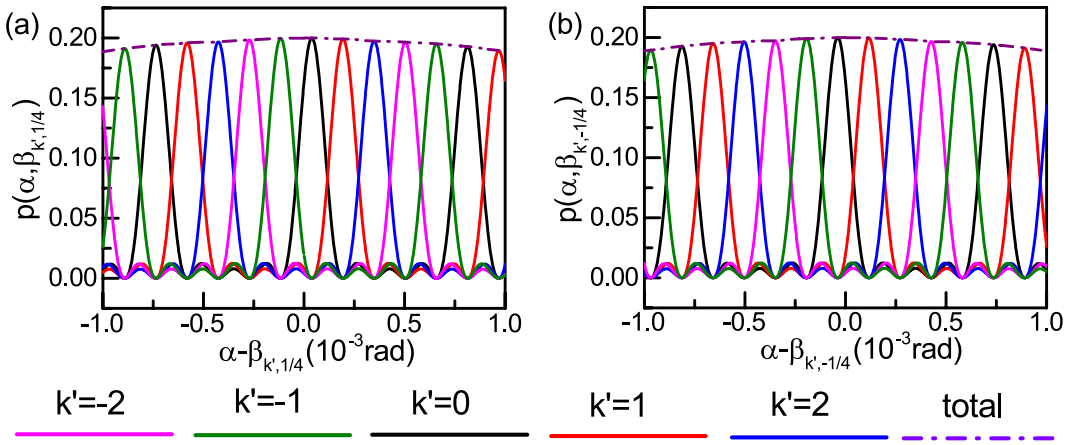

Figure 2. Joint probability $p(\alpha, \beta)$ of a 5-dimensional position-entangled two-photon state for detecting a diffracted photon in the α direction by Alice and a diffracted in the β direction by Bob. The diffracted angles for Bob are chosen as $\left(\frac{1}{4} + k'\right)\frac{\lambda}{lD}$ in (**a**) and $\left(-\frac{1}{4} + k'\right)\frac{\lambda}{lD}$ in (**b**) where $k' = -2, -1, 0, 1, 2$. The change in collecting angle for Bob shifts the pattern of the joint probability. The purple dash-dot line is the sum of all the five joint probability curves; the interference pattern appears smeared. With single-slit diffraction, its amplitude decreases as the detection angle increases.

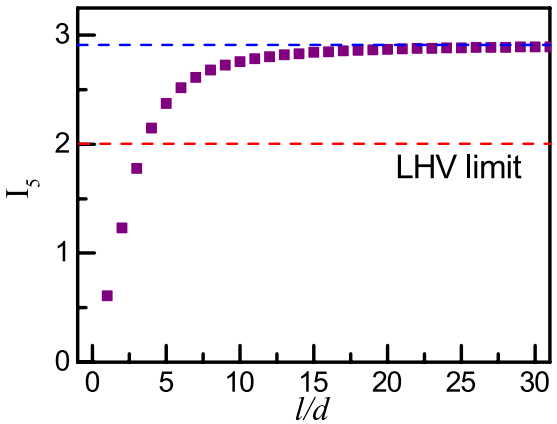

Figure 3. Theoretical Bell function I_5 versus ratio $\frac{l}{d}$ for a 5-dimensional position-entangled two photon state. With $\frac{l}{d} \leq 3$, the Bell function I_5 ceases to violate local hidden variable theorems due to single-slit diffraction; with $\frac{l}{d} \geq 10$, I_5 tends to saturate to maximal value 2.91054.

With the joint probability (Fig. 2), we are going to evaluate Bell's inequality violations, which enables us to demonstrate quantum non-locality in the 5-*D* position-entangled two-photon state. The scale factor $A^2(\alpha)A^2(\beta)$ is determined by the ratio between l and d, here we have $\frac{l}{d} = 10$. By selecting the measurement angle α as $\frac{\lambda}{ld}\left(k + 0, \frac{1}{2}\right)$, $k = -2, -1, 0, 1, 2$, and accounting for single-slit diffraction, the theoretical 5-*D* entanglement Bell function I_5 in this framework is 2.76, which is much larger than 2, the limit predicted by local-hidden-variable theories.

Discussion

We now discuss the probable influences on the Bell function. From equations (8) and (9), with fixed ratio l/d, the increase in dimension D does affect the fidelity of the Bell function. Hence the only element that may have any influence on the Bell function I_D is the ratio l/d arising from the single-slit diffraction. Because the spatial entanglement within each slit state can be neglected, the scale factor can be written as the product of the individual coefficient of Alice $A^2(\alpha)$ and Bob $A^2(\beta)$. Thus the scale factor only depends on the detection angle. For a relative large d, corresponding to a small l/d, single-slit diffraction dominates. In this case, the scale factor varies significantly within a narrow angular range which leads to a distorted joint probability curve. In contrast, as d decreases, the scale factor can be viewed as a constant for a relatively narrow range in detection angle. The measurement results approach the ideal case. From the dependence on l/d of the theoretical Bell function I_5 for 5 D entanglement(Fig. 3), I_5 for $l/d \leq 3$ ceases to violate local realism whereas it increases with l/d for $l/d \geq 10$ and asymptotes to the maximal value of 2.91054.

D	2	3	4	5	6	7	8
$l/d = 10$	2.627	2.7221	2.7322	2.759	2.7668	2.782	2.7902
$l/d = \infty$	2.8284	2.8729	2.8962	2.9105	2.9244	2.9344	2.9464

Table 1. Comparison of Bell function values I_D for $l/d = 10$ and $l/d = \infty$.

Moreover, with $l/d = 10$, we compared the Bell function I_D in simulations subject to single-slit diffraction with that for ideal cases with entanglement dimension ranging from $D = 2$ to $D = 8$; see Table 1. Here, the Bell function I_D for $l/d \to \infty$ is adopted as the value for the ideal case when considering the asymptotic behaviour of I_D with respect to l/d (Fig. 3). This table shows that the Bell function values for l/d with finite values are less than the maximal value. Furthermore, with $l/d = 10$, all values of I_D are larger than 2, which is the limit predicted by local hidden variable theorem. The Bell function values obtained here almost reach 94% of the maximal values for all dimensions. Another interesting point to note is that the Bell function values I_D, both simulated and ideal, increase with entanglement dimension D, leading to a stronger immunity to environmental noise with higher D-dimensional entanglement. This is one attractive reason for pursuing such entanglement[18].

In addition to the influence introduced by the single slit diffraction, other factors that might affect the Bell function test include inhomogeneous distribution of the pump field in the transverse plane, less precise alignment between A_2 and A_3 and the angle resolution for single photon detection. The first influence can always be found for a pump beam in the Gaussian mode, where the radial distribution of the light field is described by a Gaussian function. In this case, only a non-maximal entanglement can be generated with a consequently reduced Bell function value. Thus a plane-wave-like pump beam is needed for a larger violation of local realism theorem. The less precise alignment between A_2 and A_3 will lead to a less overlapping between the slit states of the down-converted two photons. However, such influence only causes a reduction in the coincidence counts, leaving the visibility values of the Bell kernel unaffected. The angle resolution of single photon detection $\Delta\theta$ can be written as s/f, with s the width of the single slit attached to the single-photon detectors D_s and D_i on the focal planes of L_3 and L_4 to define the spatial resolution of the detection, f the focal lengths of L_3 and L_4. A reasonable operation is to choose $\Delta\theta$ as one-twentieth of the period of the bell function in equation (8), then we have $s = \frac{\lambda f}{10lD}$. By choosing $f = 1000\,mm$ and with the values for the parameters in the above analysis, a slit width of $0.0155\,mm$ is derived for precise characterization of the Bell function curve, and this can be achieved in current experimental techniques[40].

From entanglement generation and Bell-inequality tests, we have shown in this paper that a system entangled in a Hilbert space is also entangled in its Fourier-related dual space. The joint probability for constructing the Bell function can be obtained by choosing the measurement basis vectors in the dual space. The joint probability for a high-dimensional position-entangled two-photon state was also measured in the momentum space. A similar example can be found in high-dimensional orbital angular momentum entangled two-photon states, in which the measurement of the Bell function is taken in the angular position space[9]. In addition, quantum ghost imaging, a method to obtain an image by taking the measurement of its spatial correlation, is actually a measurement of the momentum entanglement in position space[28,31]. In contrast to the assumption that the position of the photon state is a discrete variable, the momentum is a continuous variable in the measurement of the correlated diffraction. In this sense, the photon number is not conserved, and hence leads to reduced detection efficiency. However, this reduction can be compensated by adopting a sufficiently long integral time during single-photon detection.

In conclusion, we present an effective scheme to demonstrate Bell-inequality violation for a high-dimensional position entangled two-photon state. The joint probability, which is the kernel to construct the Bell function for a two-partite system entangled in a Hilbert space, can be measured by choosing a set of basis vectors in its dual space that are related by Fourier transformation. Based on the experimental configuration proposed in Pádua[40], we introduce a $4f$ system to generate D-dimensional position-entangle two-photon states, and then we analysed in detail the measurement scheme implemented for the joint probability, as well as the influence of the single-slit diffraction on the value of the Bell function. We showed that a significant violation of Bell's inequality is achievable by choosing an appropriate ratio for the distance between two adjacent slits and the width of the slit. The experimental configuration and the Bell inequality test method proposed in this paper can find a niche in performing quantum information tasks such as direct quantum communication[47] and quantum cryptography[11] where the requirement of Bell-inequality tests can be realized in momentum space while communications and quantum key distributions are established in position space.

References

1. Clauser, J. F., Horne, M. A., Shimony, A. & Holt, R. A. Proposed experiment to test local hidden-variable theories. *Physical review letters* **23**, 880 (1969).
2. Son, W., Lee, J. & Kim, M. Generic bell inequalities for multipartite arbitrary dimensional systems. *Physical review letters* **96**, 060406 (2006).
3. Horodecki, R., Horodecki, P., Horodecki, M. & Horodecki, K. Quantum entanglement. *Reviews of modern physics* **81**, 865 (2009).
4. Hensen, B. *et al*. Loophole-free bell inequality violation using electron spins separated by 1.3 kilometres. *Nature* **526**, 682–686 (2015).
5. Giustina, M. *et al*. Significant-loophole-free test of bell's theorem with entangled photons. *Physical review letters* **115**, 250401 (2015).
6. Jennewein, T., Simon, C., Weihs, G., Weinfurter, H. & Zeilinger, A. Quantum cryptography with entangled photons. *Physical Review Letters* **84**, 4729 (2000).
7. Naik, D., Peterson, C., White, A., Berglund, A. & Kwiat, P. G. Entangled state quantum cryptography: eavesdropping on the ekert protocol. *Physical Review Letters* **84**, 4733 (2000).
8. Vaziri, A., Weihs, G. & Zeilinger, A. Experimental two-photon, three-dimensional entanglement for quantum communication. *Physical Review Letters* **89**, 240401 (2002).

9. Dada, A. C., Leach, J., Buller, G. S., Padgett, M. J. & Andersson, E. Experimental high-dimensional two-photon entanglement and violations of generalized bell inequalities. *Nature Physics* **7**, 677–680 (2011).
10. Lo, H.-P. *et al*. Experimental violation of bell inequalities for multi-dimensional systems. *Scientific reports* **6** (2016).
11. Ekert, A. K. Quantum cryptography based on bell's theorem. *Physical review letters* **67**, 661 (1991).
12. Hillery, M., Bužek, V. & Berthiaume, A. Quantum secret sharing. *Physical Review A* **59**, 1829 (1999).
13. Gröblacher, S., Jennewein, T., Vaziri, A., Weihs, G. & Zeilinger, A. Experimental quantum cryptography with qutrits. *New Journal of Physics* **8**, 75 (2006).
14. Jing, J. *et al*. Experimental demonstration of tripartite entanglement and controlled dense coding for continuous variables. *Physical review letters* **90**, 167903 (2003).
15. Bennett, C. H. & Wiesner, S. J. Communication via one-and two-particle operators on einstein-podolsky-rosen states. *Physical review letters* **69**, 2881 (1992).
16. Liu, X., Long, G., Tong, D. & Li, F. General scheme for superdense coding between multiparties. *Physical Review A* **65**, 022304 (2002).
17. Braunstein, S. L. & Kimble, H. J. Dense coding for continuous variables. *Physical Review A* **61**, 042302 (2000).
18. Kaszlikowski, D., Gnaciński, P., Żukowski, M., Miklaszewski, W. & Zeilinger, A. Violations of local realism by two entangled n-dimensional systems are stronger than for two qubits. *Physical Review Letters* **85**, 4418 (2000).
19. Bruß, D. & Macchiavello, C. Optimal eavesdropping in cryptography with three-dimensional quantum states. *Physical Review Letters* **88**, 127901 (2002).
20. You-Bang, Z., Qun-Yong, Z., Yu-Wu, W. & Peng-Cheng, M. Schemes for teleportation of an unknown single-qubit quantum state by using an arbitrary high-dimensional entangled state. *Chinese Physics Letters* **27**, 010307 (2010).
21. Collins, D., Gisin, N., Linden, N., Massar, S. & Popescu, S. Bell inequalities for arbitrarily high-dimensional systems. *Physical review letters* **88**, 040404 (2002).
22. Aspect, A., Grangier, P. & Roger, G. Experimental realization of einstein-podolsky-rosen-bohm gedankenexperiment: a new violation of bell's inequalities. *Physical review letters* **49**, 91 (1982).
23. Leach, J. *et al*. Quantum correlations in optical angle–orbital angular momentum variables. *Science* **329**, 662–665 (2010).
24. Jack, B. *et al*. Holographic ghost imaging and the violation of a bell inequality. *Physical review letters* **103**, 083602 (2009).
25. Marcikic, I. *et al*. Time-bin entangled qubits for quantum communication created by femtosecond pulses. *Physical Review A* **66**, 062308 (2002).
26. Vaziri, A., Mair, A., Weihs, G. & Zeilinger, A. Entanglement of the angular orbital momentum states of the photons. *Nature* **412** (2001).
27. Pan, J.-W. *et al*. Multiphoton entanglement and interferometry. *Reviews of Modern Physics* **84**, 777 (2012).
28. Strekalov, D., Sergienko, A., Klyshko, D. & Shih, Y. Observation of two-photon "ghost" interference and diffraction. *Physical review letters* **74**, 3600 (1995).
29. Rarity, J. & Tapster, P. Experimental violation of bell's inequality based on phase and momentum. *Physical Review Letters* **64**, 2495 (1990).
30. Rubin, M. H. Transverse correlation in optical spontaneous parametric down-conversion. *Physical Review A* **54**, 5349 (1996).
31. Pittman, T., Shih, Y., Strekalov, D. & Sergienko, A. Optical imaging by means of two-photon quantum entanglement. *Physical Review A* **52**, R3429 (1995).
32. D'Angelo, M., Kim, Y.-H., Kulik, S. P. & Shih, Y. Identifying entanglement using quantum ghost interference and imaging. *Physical review letters* **92**, 233601 (2004).
33. Franson, J. D. Bell inequality for position and time. *Physical Review Letters* **62**, 2205 (1989).
34. Keller, T. E. & Rubin, M. H. Theory of two-photon entanglement for spontaneous parametric down-conversion driven by a narrow pump pulse. *Physical Review A* **56**, 1534 (1997).
35. Law, C., Walmsley, I. & Eberly, J. Continuous frequency entanglement: effective finite hilbert space and entropy control. *Physical Review Letters* **84**, 5304 (2000).
36. Kuzucu, O., Fiorentino, M., Albota, M. A., Wong, F. N. & Kärtner, F. X. Two-photon coincident-frequency entanglement via extended phase matching. *Physical review letters* **94**, 083601 (2005).
37. Hong, C. & Mandel, L. Theory of parametric frequency down conversion of light. *Physical Review A* **31**, 2409 (1985).
38. Monken, C. H., Ribeiro, P. S. & Pádua, S. Transfer of angular spectrum and image formation in spontaneous parametric down-conversion. *Physical Review A* **57**, 3123 (1998).
39. Neves, L., Pádua, S. & Saavedra, C. Controlled generation of maximally entangled qudits using twin photons. *Physical Review A* **69**, 042305 (2004).
40. Neves, L. *et al*. Generation of entangled states of qudits using twin photons. *Physical review letters* **94**, 100501 (2005).
41. Tittel, W., Brendel, J., Zbinden, H. & Gisin, N. Quantum cryptography using entangled photons in energy-time bell states. *Physical Review Letters* **84**, 4737 (2000).
42. Jha, A. K. *et al*. Angular two-photon interference and angular two-qubit states. *Physical review letters* **104**, 010501 (2010).
43. Magaña-Loaiza, O. S., Mirhosseini, M., Cross, R. M., Rafsanjani, S. M. H. & Boyd, R. W. Hanbury brown and twiss interferometry with twisted light. *Science advances* **2**, e1501143 (2016).
44. Horne, M. & Zeilinger, A. New techniques and ideas in quantum measurement theory. New York Academy of Sciences, New York **469** (1986).
45. Greenberger, D. M., Horne, M. A. & Zeilinger, A. Multiparticle interferometry and the superposition principle. *Physics Today* **46**, 22–22 (1993).
46. Greenberger, D. M., Horne, M. A., Shimony, A. & Zeilinger, A. Bell's theorem without inequalities. *American Journal of Physics* **58**, 1131–1143 (1990).
47. Deng, F.-G., Long, G. L. & Liu, X.-S. Two-step quantum direct communication protocol using the einstein-podolsky-rosen pair block. *Physical Review A* **68**, 042317 (2003).

Acknowledgements

This work was supported by Young fund of Jiangsu Natural Science Foundation of China (SJ216025); National fund incubation project (NY217024); Scientific Research Foundation of Nanjing University of Posts and Telecommunications (NY215034). We thank Richard Haase, Ph.D, from Liwen Bianji, Edanz Group China (www.liwenbianji.cn/ac), for editing the English text of a draft of this manuscript.

Author Contributions

Wei Li devised the theoretical scheme, and provided the theoretical analysis. Wei Li and Sheng-Mei Zhao co-wrote the paper.

Additional Information

Competing Interests: The authors declare no competing interests.